PRACTICAL APPLICATION OF LIQUEFACTION ON LONG BEACH SANDS

A THESIS

Presented to the Department of Civil Engineering and Construction Engineering Management

California State University, Long Beach

In Partial Fulfillment

of the Requirements for the Degree

Master of Science in Civil Engineering

Committee Members:

Luis G. Arboleda-Monsalve, Ph.D. (Chair)
Tesfai Goitom, Ph.D.
Lisa Star, Ph.D.

College Designee:

Antonella Sciortino, Ph.D.

By Armando Murillo Jr.

B.S., 2012, California State University, Long Beach

January 2017

ABSTRACT

PRACTICAL APPLICATION OF LIQUEFACTION

ON LONG BEACH SANDS

By

Armando Murillo Jr.

January 2017

This thesis presents the construction sequence of a liquefaction tank for simulating liquefaction for observation and laboratory testing. The project consists of constructing an acrylic tank to hold sand, a water reservoir, casting a porous stone to allow even water distribution, installing a pipe system and pump for water flow, manufacturing lateral support braces, and modifying a steel cart to install the whole assembly.

Sand collected from Junipero Beach within the city of Long Beach is used as the testing media in the tank. Sand collected at this location shows favorable liquefiable gradations and is located within a liquefaction hazard zone. Laboratory testing using the proposed liquefaction tank demonstrated that this apparatus is functional and able to induce liquefaction on the sample of Long Beach sand.

ACKNOWLEDGEMENTS

I would like to give thanks to my family for supporting me throughout college to further my education and to pursue my goals. I would like to thank my advisor Dr. Luis G. Arboleda-Monsalve for his guidance, patience with my busy work schedule, and insight into this project. I would like to thank Dr. Tesfai Goitom and Dr. Lisa Star for taking time in being part of my thesis defense committee. I would like to thank my employers Steve Tsai and Marsha Ramos at Geosystems for being flexible with my work schedule to allow me to finish my thesis project. Lastly, I would like to thank California State University, Long Beach Alumni Association for their financial assistance through the Alumni Grant for making this project possible.

TABLE OF CONTENTS

LIST OF TABLES

LIST OF FIGURES

CHAPTER 1

INTRODUCTION

1.1 Introduction

Earthquakes cause damages to infrastructure and negatively affect society with major economic losses and fatalities. The majority of damages are caused by landslides, floods, tsunamis, structural damages, or can sometimes be attributed to soil liquefaction induced by earthquakes. Great interest rose in trying to understand the liquefaction phenomenon after a string of earthquakes in 1964 that caused major liquefaction related damages to structures and land in Alaska and Japan. Since then major advances have been made in coming up with methods to predict and reduce the susceptibility of soil to liquefy.

Sand is the most prominent soil type that is susceptible to liquefaction under fully saturated conditions. Loose saturated sand subjected to cyclic loading during an earthquake transfers its seismic stresses to the surrounding water in the soil structure, generating excess pore water pressures. When the soil structure cannot dissipate the excess pore water pressure, it leads to a reduction in effective stress and in turn the loss of shear strength. This loss of shear strength causes differential settlements in the soil leading to damages to structures.

Liquefaction damages manifest itself in different ways. One of the ways to tell if liquefaction occurred in an area is by seeking the presence of sand boils. Sand boils occur when excess pore water pressure causes groundwater to flow towards the surface with sand particles. Sand boils were observed during the 1989 Loma Prieta earthquake in Oakland, California, and the 1979 Imperial Valley earthquakes in Imperial County, California, as shown in Figure 1.

FIGURE 1. Sand boils generated after the earthquake. (left) 1989 Loma Prieta earthquake; (right) 1979 Imperial Valley earthquake.

Cases of liquefaction began to be recorded in higher detail after a string of earthquakes starting in 1964 with the Good Friday earthquake with magnitude of 9.2 in Alaska and the Niigata earthquake with magnitude of 7.5 in Japan occurred. Major structural damage was observed and documented in these cases. Numerous case histories show damages caused by liquefaction, which include settlements of structures, foundation failures, lateral spreading, flotation of underground utilities, and failure of retaining walls. Liquefaction induced damages occurred in the 1999 Kocaeli earthquake in Turkey and the 1964 Niigata earthquake in Japan where foundations failed due to bearing capacity failure when soil liquefied, as shown in Figure 2.

FIGURE 2. Bearing capacity failure due to differential settlement. (left) 1999 Kocaeli earthquake; (right) 1964 Niigata earthquake.

The most destructive form of liquefaction is lateral spreading. Lateral spreading is the flow of soil down an inclined plane in the soil layer. When there is a liquefiable layer of soil in an inclined surface we see large masses of earth flow down the plane along with any structures or foundations located on the soil mass. Common damages are settlements of structures with permanent displacement of large bodies of earth. This type of damage tends to be found near large bodies of water. Lateral spreading is most damaging to bridges' and buildings near waterways as liquefaction causes permanent displacement of the bridges foundations and soil masses, as shown in Figure 3. Lateral spreading caused bridge spans to fall off their supports during the 1964 Niigata earthquake and a whole residential area to be permanently displaced along the slope during the 1999 Kocaeli earthquake.

FIGURE 3. (left) Fallen bridge spans caused by lateral spreading during the 1964 Niigata earthquake. (right) Lateral spreading of waterfront properties during the 1999 Kocaeli earthquake.

Liquefaction can also cause major damage to underground utilities by permanently displacing them from their original location. During an earthquake, large buoyant forces are generated by underground utilities that cause them to move towards the surface. This is critical in urban environments as damages to gas lines, sewers, water pipes, and utilities can pose many dangers, as shown in Figure 4 during the 2004 Chuetsu earthquake.

FIGURE 4. Flotation of sewage lines during 2004 Chuetsu earthquake.

Retaining systems can be prone to major failures during earthquakes if located in liquefiable soils. Liquefaction can decrease the passive pressures and increase the active pressures in retaining systems such as retaining walls and earth dams. Flow failures have caused damages in earth dams and other slopes where flow is driven by gravitational force during liquefaction. During 1971, a portion of the San Fernando dam collapsed causing large portions of earth to flow into the dam when the retaining soil liquefied, as shown in Figure 5.

FIGURE 5. San Fernando Dam failure during 1971 San Fernando Earthquake.

1.2 Objective

The goal of the proposed project is to build a sand tank to observe experimentally the changes in the properties of a sand layer subjected to liquefaction. Even though the idea of constructing a sand tank to illustrate the liquefaction phenomenon is not anything new, the

demonstration tends to last in the student's mind and triggers their interest in the causes and consequences of this phenomenon. The construction of this tank will inspire students and faculty in the engineering department with a vivid demonstration of the phenomenon that causes damage to infrastructure in earthquake prone areas. In the future, once the first prototype has been built and tested, the scope of work of the tank will be expanded for partially saturated soils to study the influence of the degree of saturation in the liquefaction resistance of gassy soils and to study the behavior of laterally loaded piles in biocemented sands used as a liquefaction mitigation alternative.

CHAPTER 2

TECHNICAL BACKGROUND

2.1 Background

Liquefaction induced failures have been extensively documented since the 1964 Niigata and Alaska Earthquake. Since that time the documentation of earthquake induced liquefaction has grown to include liquefaction related failures during the 1990 Dagupan (Philippines), 1999 Chi-Chi (Taiwan), 1999 Kocaeli (Turkey) earthquakes, and more recently during the 2010 and 2011 Christchurch (New Zealand) earthquake. Much progress has been achieved thus far in understanding the causes behind liquefaction and in developing methods to better predict and mitigate the susceptibility of soils to liquefy.

Characteristics of sandy material change depending on its properties such as relative density, degree of saturation, and if it is subjected to static or dynamic loadings. Liquefaction occurs when the right mixture of soil properties and dynamic loading occur simultaneously. The mechanical behavior of liquefaction can be explained based on the principle of effective stress, taught in introductory soil mechanics courses. When fully saturated sand is subjected to rapid dynamic loadings, usually caused by earthquakes, there is an increase in pore water pressure in the soil body. This buildup of pore water pressures, known as excess pore water pressure, are caused when water cannot dissipate the excess pressures it is being subjected to. This excess pore water pressure reduces the effective stress of the soil thus reducing its shear strength. At the point of failure due to this loss of soil strength we see the soil mass liquefy as water takes on the load and it is then that we see failures as buildings start to sink into the soil and buried utilities float up to the surface. Once dynamic loads subside, excess pore water pressures dissipate and the soil mass regains its shear strength and reconsolidates.

2.2 Factors Affecting Liquefaction Susceptibility

The factors that influence the liquefaction susceptibility of sands are the grain size distribution, soil type, relative density, effective stress, geologic history, and degree of saturation. Tsuchida (1970) proposed boundaries of grain size distribution for liquefiable soils to aid in identifying them, as shown in Figure 6. This chart shows that sandy gradations are the most liquefiable type of soil.

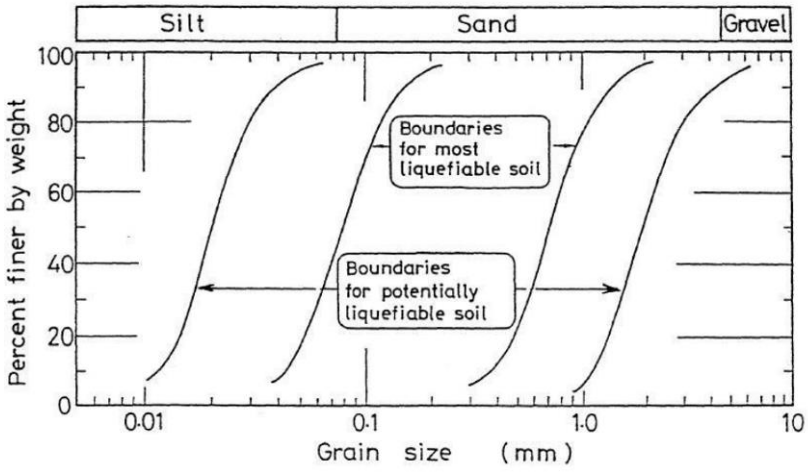

FIGURE 6. Grain size distribution of liquefiable soils (Tsuchida 1970).

Liquefaction potential of dense soil is less than that of those of loose soil. The void ratio and the contractive or dilative behavior of the soil has a major influence in liquefaction susceptibility. Dense sands are less prone to liquefaction because their low void ratio is located below the critical void ratio line and negative excess pore water pressures generated as the soil dilates during shearing tends to increase the effective stress, inhibiting liquefaction. Loose sands are more prone to liquefaction as they have higher void ratio, which is above the critical void ratio line. Loose soils have contractive behavior during shearing which generate positive excess pore water pressures which decrease effective stresses. Critical void ratio (CVR) line

(Casagrande 1936) sets the boundary of soils susceptible to liquefaction depending on the void ratio (e) and effective confining pressures (σ'_{3c}), as shown in Figure 7.

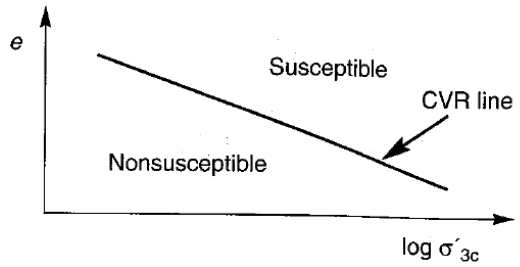

FIGURE 7. Critical void ratio line as a boundary of contractive and dilative states to assess liquefaction susceptibility (Kramer 1996).

It has also been discovered that saturated sands located deeper than 15 to 18 meters are not likely to liquefy. This is because vertical effective stresses increase with depth and at certain point not enough shear stress is generated to induce liquefaction. Geology plays an important role as well, younger sand deposits tend to have lower shear strength due to a lack of sufficient cementation and densification caused by aging and being in a loose of critical state form that make them more susceptible to liquefaction. In contrast, older alluvial deposits are denser and have more natural cementation which makes them less susceptible to liquefaction.

2.3 Other Prototypes of Liquefaction Tanks

The construction of a liquefaction tank has been addressed from varying viewpoints and different prototypes have been built in other schools of engineering and research facilities. The original tank this project took inspiration from was built at Northwestern University and has been replicated at the University of Illinois, the Nyang Technological University in Singapore, and California State University Pomona, just to cite a few. Holtz et al. (2010) presented the first model of a sand tank that was built in Northwestern University (Evanston, IL). The principal investigator of this proposal had the opportunity to use the tank for numerous demonstrations of the liquefaction phenomenon in the classes of introductory soil mechanics. The tank model is

composed of a tank containing sand loose of critical state and a water reservoir, as shown in Figure 8. A pump is use to inject water from the reservoir into the tank creating an upward flow, which is a necessary but not sufficient condition to induce liquefaction in the soil. A porous stone installed at the bottom of the tank uniformly distributes the water pressure along the soil mass. The injection of water flow increases the pore water pressure and acts as a lubricant between soil particles making the soil mass more susceptible to liquefaction. This increase in pore water pressure are measured with piezometers installed along the walls of the tank.

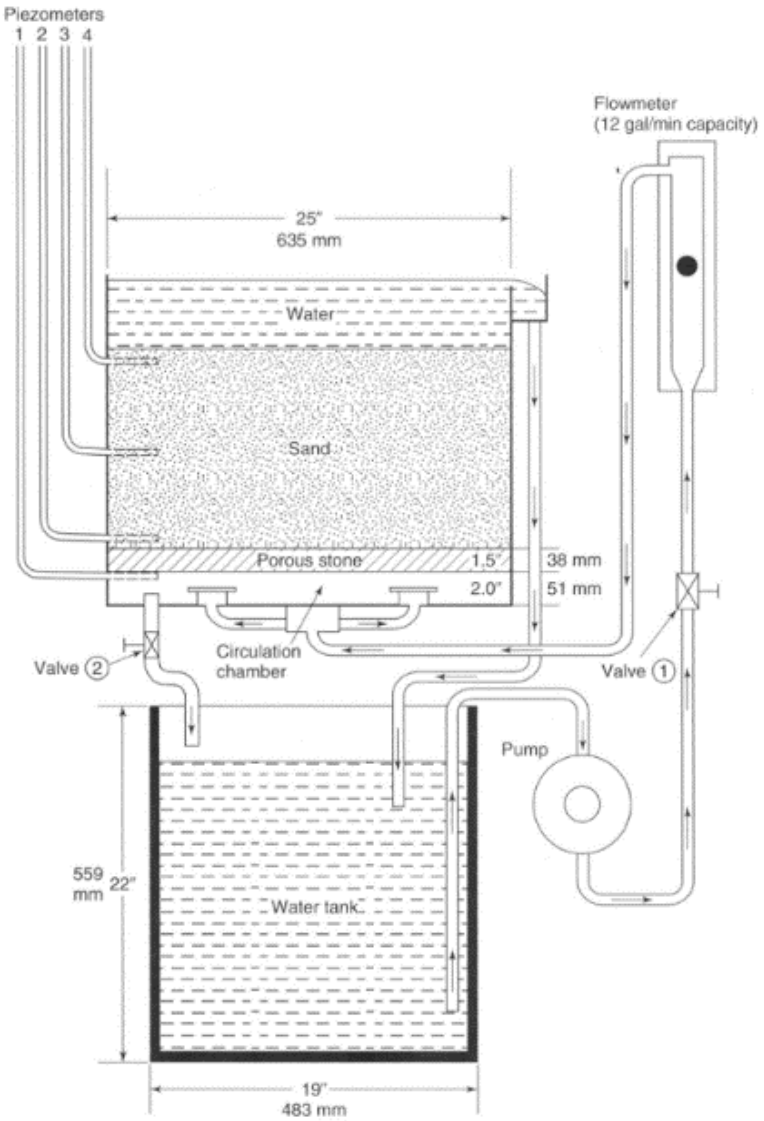

FIGURE 8. Liquefaction tank (Holtz et al. 2010).

CHAPTER 3

CONSTRUCTION SEQUENCE

3.1 Liquefaction Tank Schematic

The liquefaction tank build for this project is based off the sand tank that was built at Northwestern University as presented in "Introduction to Geotechnical Engineering" by Holtz et al. (2010). The original schematic shows all the main components that are needed to build a working model, as shown in Figure 8. The main components needed are a container to hold the sands, a water reservoir to store water, a water pumping system, piezometers to measure water pressure inside the tank, a flowmeter to measure water flow rate into the tank, and water drains. Construction of the liquefaction tank was performed in a functional and cost-effective manner. All tools used are easily obtainable to encourage other institutions to build a liquefaction tank as an educational aid to educate upcoming engineers and bring interest to students in pursuing careers in the fields of STEM (Science, Technology, Engineering, and Mathematics) through this interesting phenomenon.

3.2 Sand Tank

The tank needs to be constructed of a stiff and durable material that can hold sand and water. It needs to be transparent so that students see the liquefaction phenomenon and loss of bearing capacity in sands. For these reasons the tank was built out of 1.9 cm thick clear acrylic sheets to allow visibility of the whole system and have ample strength to support all pressures. The outer dimensions of the tank were built to be 60 cm by 60 cm by 80 cm.

The first step in building the tank is to mark all measurements needed for the five acrylic sheets that are to be cut. Five 1.9 cm thick acrylic sheets were used for the tank construction. The bottom portion is cut to 60 cm by 60 cm, then two sheets are cut to 60 cm by 80 cm, and finally

the last two sheets are cut to 56 cm by 80 cm to account for wall thickness. A measuring tape, angle square, and a straight edge level are used to mark all measurements and to insure the markings are squared and straight, as shown in Figure 9.

FIGURE 9. Working table preparations for marking required measurements for wall cuts.

FIGURE 10. Table clamps used to secure acrylic boards during cutting.

The acrylic sheets need to be secured in position as they can move from their position by vibrations and force applied by the cutting saw during cutting leading to crooked cuts. Securing the acrylic sheets by using table clamps resolves this problem and prevents them from moving

during the cutting process. A straight edge from an acrylic board was clamped over the board to be cut to serve as a guide for the circular saw, as shown in Figure 10 and Figure 11. This guide helps in making the cut straight over long cutting distances when using a circular saw. Enough saw blade clearance is needed at the bottom of the sheet to be cut to prevent saw blade and working surface damage. This can be accomplished by either hanging the sheet over the side of the table or elevating it by using spacers.

FIGURE 11. Side view of clamped acrylic sheets.

FIGURE 12. Acrylic sheet cut to the required length.

In absence of a table saw, a handheld circular saw was used to make all straight cuts on the acrylic sheets, as shown in Figure 12. A plastic cutting saw blade was used to ensure smooth and clean cuts. It is important to use a circular blade design for cutting acrylic as it will make cleaner cuts. Using an improper blade for the material can lead to the material getting chipped or causing the blade to break, leading to personal injury.

FIGURE 13. Table jig to create a squared inclined surface.

After performing all the cuts, the next step is to glue all the sheets together. A squared jig was made to ensure that the sheets are glued perpendicular to each other. The construction jig base consists of 18 cm long piece of 10 cm by 15 cm timber piece drilled perpendicularly onto the flat surface of the working table using an angle square, as shown in Figure 13. This jig is very helpful in making sure that the bonding surfaces are squared to each other and works as an aid to hold two surfaces together as the epoxy cures. Bonded surfaces can be left on the inclined table jig after the initial epoxy hardening period without worry that the sheets will fall without manually holding them by hand. They are held in place by their own weight.

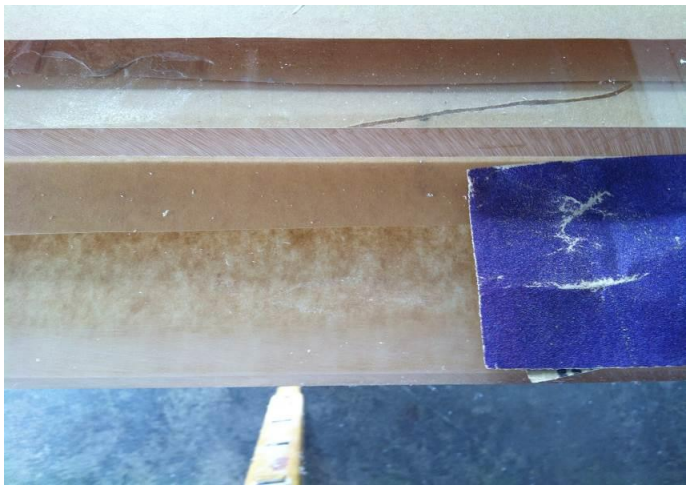

FIGURE 14. Mating surface sanded for proper gluing contact.

All surfaces that were to be glued were first sanded before adding epoxy to ensure a strong bond between all contact surfaces. Good contact is needed for epoxy to bond well with its mating surface. Glue bond shear failure can occur if the mating surface is too slick for the glue to penetrate and bond with. Acrylic sheets are polished from the factory and offer a bad bonding surface, which is fixed by sanding down the bonding surfaces prior to gluing, as shown in Figure 14.

FIGURE 15. First wall glued together on the inclined work table.

The first wall is glued on the inclined table and jig to hold it in place during the glue curing period, as shown in Figure 15. Minor adjustments are made during the initial glue handling period to align the edges of the sheets and to check if the walls are perpendicular to each other using an angle square. Once the epoxy hardened, it is left to cure for 24 hours before any additional handling.

FIGURE 16. Gluing of second wall.

FIGURE 17. Gluing of third wall.

The same procedure is followed for second and third walls, as shown in Figure 16 and Figure 17. For the other walls the tank is rotated against the table jig for the next wall to be glued and left to cure 24 hours before additional handling and gluing of subsequent wall.

FIGURE 18. Gluing of bottom acrylic sheet.

Lastly, the tank is flipped up and the bottom acrylic sheet is glued to the top, as shown in Figure 18. The bottom base is held in place by its own weight as the epoxy cures. Once the tank was finished, silicon was used on all inner and outer edges to waterproof the tank.

3.3 Cart

The goal behind the construction of this liquefaction tank is that it should be able to be mobile to allow ease of transport for demonstrative purposes. In order to accomplish this goal, it was decided that it should be constructed on a strong enough cart to handle all the weight from the tank, sand, and water. A pre-manufactured steel cart with high weight capacity was purchased to fill this need, as shown in Figure 19. The cart comes with built-in factory reinforcements that allow the shelves to have a much higher weight capacity, as shown in Figure 20.

FIGURE 19. High weight capacity steel cart.

FIGURE 20. Bottom shelves reinforced with steel beams.

3.3.1 Modifications to Cart

Some minor modifications were performed on the cart to allow for the installation of a steel base to hold the tank and two holes for the installation of water drains. An electric drill with an 80 mm steel drilling drill bit was used along with drilling oil to drill holes in the midsection

area of the cart to create holes to bolt on a base to hold the tank onto the cart, as shown in Figure 21.

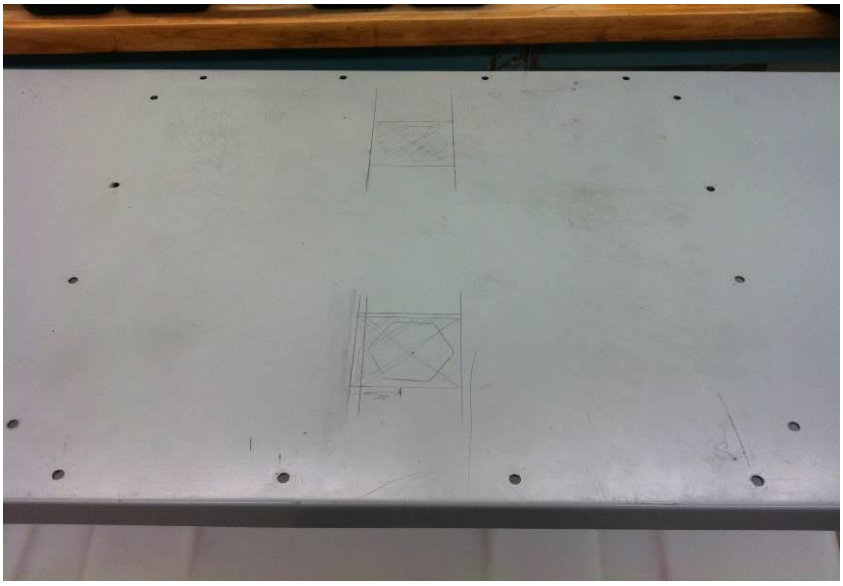

FIGURE 21. Drilled holes on top of cart shelve for installing base to hold tank onto the cart.

Two holes were needed through the top cart shelve to install a tank drain and a waterline into the tank. These were marked onto the cart using the actual drain to determine proper cutting size to allow for handling of drain and pipes during installation. An angle grinder with a steel cutting disk was used to cut the two square holes, as shown in Figure 22. The cuts were deburred with a grinding wheel and a file to get rid of sharp edges left behind by cutting that may lead to cuts during handling. During the cutting and drilling process the midsection received many scratches and left sections of bare steel exposed. This area was repainted to protect the steel from rust.

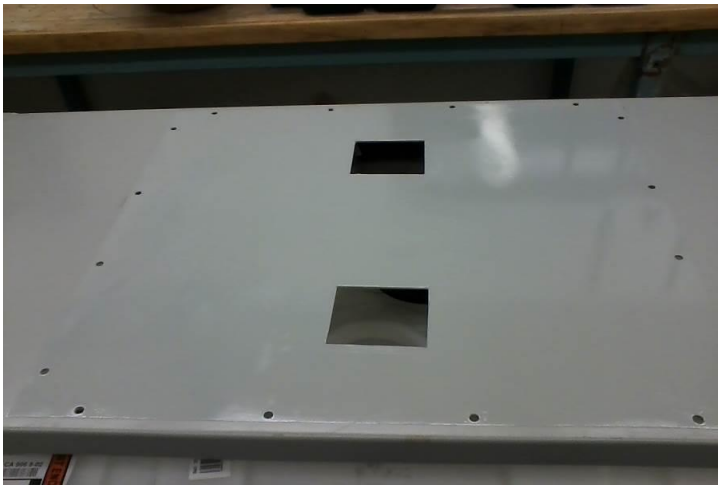

FIGURE 22. Square holes for the installation of a drain and water pipe.

3.4 Tank Holding Base

A base is needed to attach the tank on top of the cart to hold it in place during testing and transportation. This base was manufactured out of angle steel with a web of 5 cm to allow enough webbing from the steel to hold the tank in place, as shown in Figure 23. The manufacturing process for this base required four pieces of angle steel cut to a length of 62 cm. A miter saw with a steel cutting blade was used to make these cuts. An extra 1.5 cm tolerance was given to account for material loss from cutting and cutting imperfections from using a miter saw.

FIGURE 23. Angle steel for tank base prior to cutting.

The ends of all the angle steel were cut to 45 degrees using the miter saw angle measure, as shown in Figure 24. They were cut to 45 degrees so they can be welded into a square base.

FIGURE 24. Angle steel ends cut to 45 degrees to allow for welding of a square base.

FIGURE 25. Welded base on the cart prior to hole drilling.

The base was welded using an arc welder using 6013 electrodes, which are appropriate for general purpose welding and pre-fitted onto the cart, as shown in Figure 25. After welding was completed, the base was drilled with an electric drill using an 80 mm steel drilling drill bit to

make holes to bolt the base. A combination of an 80 mm bolt, pressure washer, and nut was used for every drilled hole. Using a pressure washer is essential in this bolting combination as it helps to prevent the nuts from becoming loose due to vibration.

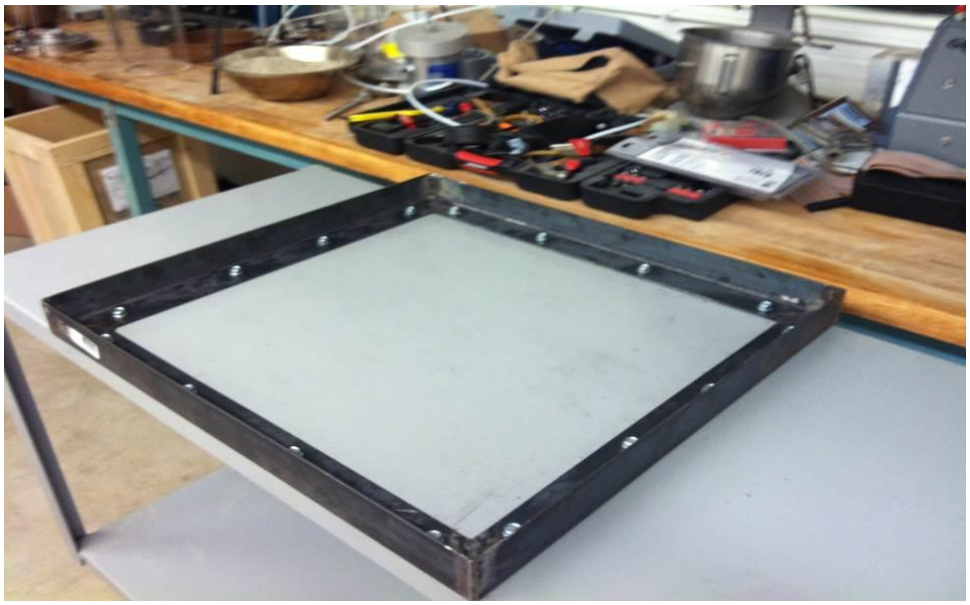

FIGURE 26. Base fitted and bolted onto the cart prior to painting.

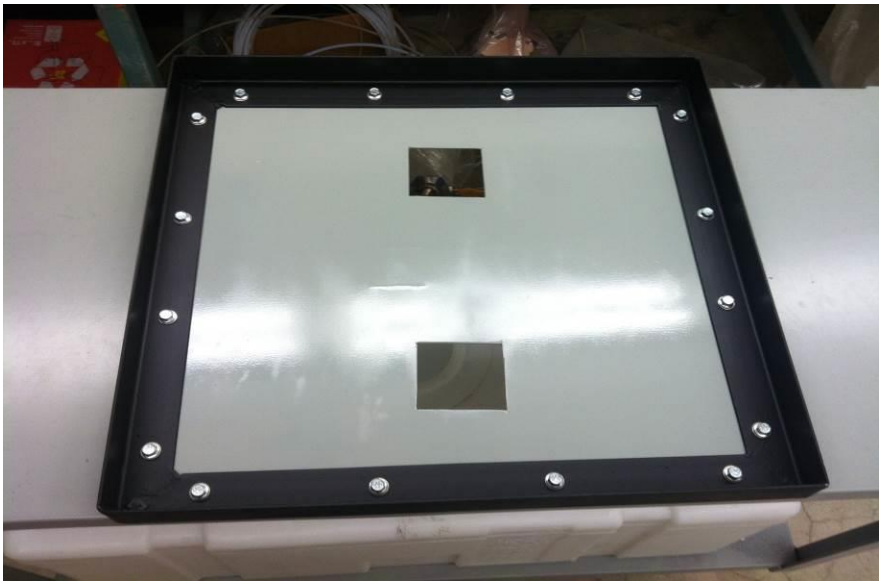

FIGURE 27. Finished painted base attached to the cart.

When the fitting was finished, the base was removed from the cart for painting, as shown in Figure 26. Painting the base is necessary as to prevent the metal from rusting. First a primer base was used to paint the base as to provide a tight bond for the subsequent paint layers. After the primer dried, the base was spray painted using two coats of black paint for metallic surfaces. The finished painted base, which is bolted onto the cart, is shown in Figure 27 and a close-up of the tighten bolts is shown in Figure 28.

FIGURE 28. Close-up of bolts on the surface.

3.5 Support Braces

Varying horizontal forces are going to be exerted on the liquefaction tank stemming from the earth pressures from the sand, water pressure, and active loads during testing. There is a potential that the glue bonds may fail in the future due to fatigue or excessive applied loading during testing. Exterior support braces were manufactured to provide additional lateral support to the tank and to double as a safety device if a glue bond were to fail. They would hold the tank walls together and keep the sands in place only allowing water to escape through any cracks if

any were to develop with time. The braces were manufactured out of angle steel with a 2.5 cm webbing, as shown in Figure 29.

FIGURE 29. Angle steel for braces with a 2.5 cm web.

FIGURE 30. Angle beams to be cut for manufacturing of support braces.

Four steel angle beams were cut to a length of 76 cm with an angle grinder with steel cutting disk for each corner of the tank, as shown in Figure 30. To connect all beams together a system of ties and tie holders were manufactured. The tie holders were manufactured from 2.5

cm wide by 6.4 cm flat piece of steel to create tabs where lateral steel ties would be installed to fasten the bracing structure to the tank, as shown in Figure 31.

FIGURE 31. Flat steel beam used to make tabs for retaining structure.

A total of 16 flat steel tabs were cut for making tie holders, as shown in Figure 32. All tabs were drilled with an electric drill with steel drilling bit to allow for the tie rod to go through the opening for bolting. Each angle beam has four tabs per beam to allow two tie rods to be installed on each side of the outer portions.

FIGURE 32. 16 flat steel tabs for the installation of tie rods.

FIGURE 33. Welded braces.

After the tabs were cut and drilled, they were welded on to the beams using 6013 electrodes on an arc welder. Angle beams were numbered and measured before welding to ensure the steel tabs were welded in correct order and position. The tabs were welded and grinded to remove slag and excess welding material, as shown in Figure 33. Braces were primed first before being painted with two coats of paint for steel to prevent rust.

FIGURE 34. Braces fitted onto the tank prior to installation of tie rods.

Masking tape was used to hold the braces in place while the tie rods were installed and fitted, as shown in Figure 34. Some fitting was necessary on the tie rods as they were too long from factory, as shown in Figure 35. The right side of the image shows the tie rod overhang that needed to be trimmed. An angle grinder was used to cut off excess material while taking precaution not to damage the threads on the tie rods.

FIGURE 35. Tie rods installed on the braces with excess material overhang prior to trimming.

FIGURE 36. Close up of tie rod ends with bolting combination.

These tie rods were bolted using a combination of a washer, pressure washer, and a nut at each end, as shown in Figure 36. The pressure washers were used to aid in preventing the nut from becoming loose due to vibrations. With these nuts the tension on the rods can be adjusted by tightening or loosening them.

3.6 Porous Stone

The porous stone serves the purpose of distributing water flow evenly across the surface area of the tank and preventing sand from being drained back into the water reservoir. The porous stone was made of a mixture of only pea gravel and Portland cement to make it permeable. There was a lack of information regarding mixture ratios to make permeable concrete. Test samples were tested at different cement, aggregate, and water contents to come up with a mixture that would be permeable to water. In the sample mixtures, it was found that excluding sand in the mixture allowed the cement to be porous enough to allow water to be filtered through the stone at a fast-enough flow rate. Including sand led to samples that were impermeable using a standard mixture of aggregate, cement, and water. From test samples, it was found that adding enough Portland cement so that the aggregate is covered with it produced more permeable stones. Small amounts of water were added and mixed until the cement was moist. Making the mixture too wet lead to the pores to become clogged with cement and make the sample impermeable.

The first step in creating the porous stone was to build a mold with inner measurements of 56 cm by 56 cm out of wood with a wooden base to hold the mixture, as shown in Figure 37. These measurements would allow for enough clearance to insert the stone into the tank during installation.

FIGURE 37. Mold for casting of porous stone.

FIGURE 38. Galvanized steel mesh to resist corrosion from water.

Galvanized steel mesh was used to reinforce the porous stone and to prevent the stone from cracking during handling due to the lack of sand in the mixture. This material was chosen due to its higher resistance to corrosion in water. Two sheets were cut with an angle grinder to the dimensions of 56 cm by 56 cm from a bigger sheet, as shown in Figure 38.

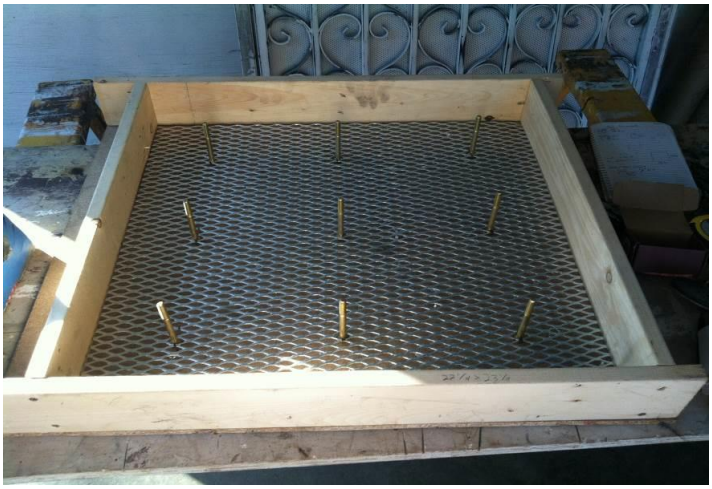

FIGURE 39. Mold with steel mesh and bolts install in the lower portion.

The galvanized steel mesh is placed in the mold with nine 80 mm threaded bolts installed thorough the bottom mesh, as shown Figure 39. These bolts are used to secure the bottom and top wire meshes together once the cement mixture was poured into the mold.

FIGURE 40. Concrete mixture with sufficient Portland cement to coat the aggregate.

The mixture was mixed with enough Portland cement to cover the surface of the gravel and enough water to create a moist mixture, as shown in Figure 40. As stated earlier, it was discovered from test sample mixtures that using large amounts of Portland cement or water during mixing created a stone that is impermeable. This is due to excess cement settling at the

bottom or a mixture that is too wet that it drains most of the cement to the bottom of the mixture and clogs the pores in both cases.

FIGURE 41. Mixture casted into mold.

FIGURE 42. Steel mesh added to top of mixture.

Water was added in small quantities and mixed until the mixture was moist. Once the concrete mixture was ready, it was poured into the mold and smoothened to a flat surface, as shown in Figure 41. The top layer of the steel mesh was added to the top of the mixture to check for bolt alignment before the mixture hardened and adjusted accordingly, as shown in Figure 42.

The mold was filled with water and the concrete was left to cure for a week. The mold was refilled with water during the week whenever the water level drop.

FIGURE 43. Finished porous stone.

Once the concrete mixture cured, the two steel meshes were bolted together with the pre-installed bolts that were added to the bottom wire mesh. A pressure washer and nut combination was used to bolt together the two steel meshes above and below the porous stone. A set of chains was installed on the porous stone using the bolt heads to allow ease of installation when handling the stone, as shown in Figure 43. Silicon was added to the side areas of the porous stone to prevent raveling.

Finally, a perforated base was made of acrylic to the dimension of 51 cm by 51 cm by 5 cm and glued together with epoxy, as shown in Figure 44. This base was used to seat the porous stone inside the tank and to allow water to be distributed evenly before reaching the porous stone.

FIGURE 44. Base to sit the porous stone inside the tank.

3.7 Pipe System

Water is necessary to induce liquefaction. This goal is accomplished by building a network of pipes to pump and drain water from the liquefaction tank. A tank was purchased and installed in the lower shelf of the cart to act as the water reservoir. Water is pumped into the liquefaction tank using a 2-horse power pump installed in the lower outside wall of the reservoir tank. This pump has a maximum flow rating of 26.5 liters per minute and is attached to the water

FIGURE 45. Hole drilled on side of reservoir tank for installation of pump inlet.

reservoir via a pipe and nut. A 1.9 cm hole was drilled on the side of the reservoir tank to act as the point to install an inlet for the pump, as shown in Figure 45. The pump was inserted into this hole with rubber seals on both sides of the wall connections with the pipe to prevent water from leaking, as shown in Figure 46.

FIGURE 46. Nut and rubber seal used inside of water reservoir to install pump inlet.

FIGURE 47. Water pump connected to the tank and outlet pipe installed with plastic coupling.

After attaching the pump to the water reservoir, the pump was then connected to a 1.3 cm diameter pipe for outflow using a plastic coupling to avoid damage of the pump threads, as shown in Figure 47.

FIGURE 48. Flowmeter for measuring water flow rate into the liquefaction tank.

Next in the pipe system is the installation of the flowmeter, as shown in Figure 48. The flowmeter was installed to measure the rate of water flowing into the tank. A yellow valve installed next to the flowmeter controls the flow going into the tank, as shown in Figure 49. By adjusting this valve, the flow rate can be adjusted to any desired flow from zero to 26.5 liters per minute.

After the flow controlling valve, a 1.9 cm diameter pipe is connected into the tank using a wall fitting, as shown in Figure 50. This is installed by first drilling a hole into the bottom of the tank, through the square hole previously cut into the cart, to install the fitting and then connecting the pipe. This last connection completes the pipework for the water flowing into the liquefaction tank.

FIGURE 49. Valve installed to control rate water flow into liquefaction tank.

The drain system is simple in its layout and construction. The drain is installed onto the same type of wall fitting used previously. A hole is drilled on the acrylic sheet through the bottom square opening, previously cut into the cart, at the bottom of the liquefaction tank to install the wall fitting. After installing a pipe onto the wall fitting, a red valve is installed to control water drainage from the bottom of the tank. More pipes are connected using couplings after the valve to divert water into the water reservoir, as shown in Figure 51.

FIGURE 50. Inlet flow pipe connected to wall fitting.

FIGURE 51. Tank drainage pipe system with control valve.

When conducting liquefaction tests there is the possibility of water overflowing over the tank. An overflow pipe drain was installed above the sand surface to prevent water from overflowing through the top of the tank, as shown in Figure 52. This pipe drain was installed using the same type of wall fitting used in the bottom of the tank. A coupling is connected from the wall fitting to install a long pipe to bring overflow water back into the reservoir in the lower cart shelf, as shown in Figure 53.

FIGURE 52. Overflow pipe connected to wall fitting.

FIGURE 53. Long pipe connected to wall fitting to bring overflow to water reservoir.

Additional couplings and pipes were used at the bottom of the tank to direct overflow water straight into the water reservoir. The overflow pipe drain into the same entrance to the water reservoir as the drain at the bottom at the tank, as shown Figure 54.

FIGURE 54. Overflow drain directed into water reservoir.

3.8 Piezometers

A piezometer is a device that is used to measure pore water pressure by measuring the height to which water rises along the water column. It is important to see the changes in water

pressure as liquefaction occurs due to the increase in these pore pressures. Five piezometers were installed along the wall of the tank to monitor water pressures during testing. Three were installed on one side of the tank and two more were installed on the opposite of the tank to monitor if there are any differences in pore water pressure across the tank.

Five holes were drilled along the wall of the tank to install piezometers using an electric drill with a hole saw bit. Pilot holes were drilled prior to using a saw to drill perpendicular to the wall, as shown in Figure 55. The piezometers were installed after drilling, as shown in Figure 56. The piezometer connection used on this tank consists of a pipe, rubber washers, hose nipple, and nut.

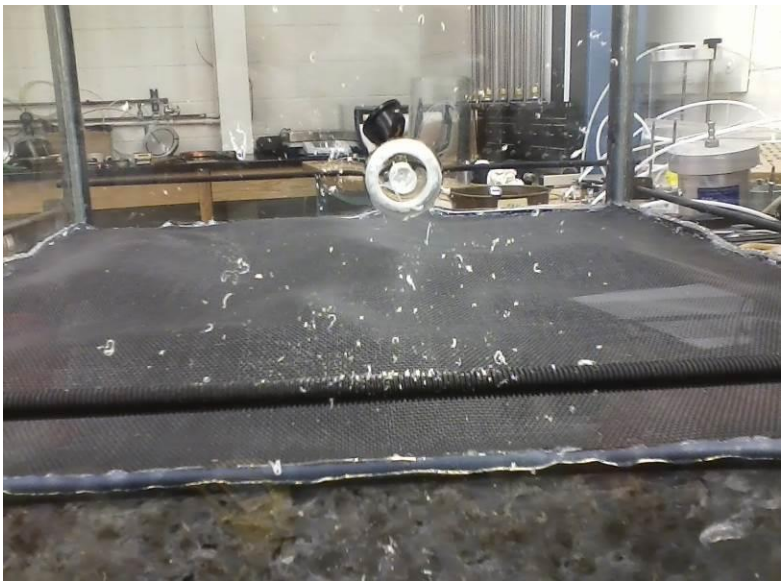

FIGURE 55. Holes being drilled for piezometers.

Clear tubing is then connected to the five piezometers wall connections and tighten to the nipples using hose clamps to hold the hoses in place, as shown in Figure 57. The hoses are then attached to a board with rulers that serve the purpose of measuring the height of the water column during testing. The piezometers are attached to the tank using a latching hook that hooks

into the support braces, as shown in Figure 58. This final step concludes the construction sequence of the liquefaction tank.

FIGURE 56. Piezometer connection installed on the wall of the tank.

FIGURE 57. Side view of wall with piezometers.

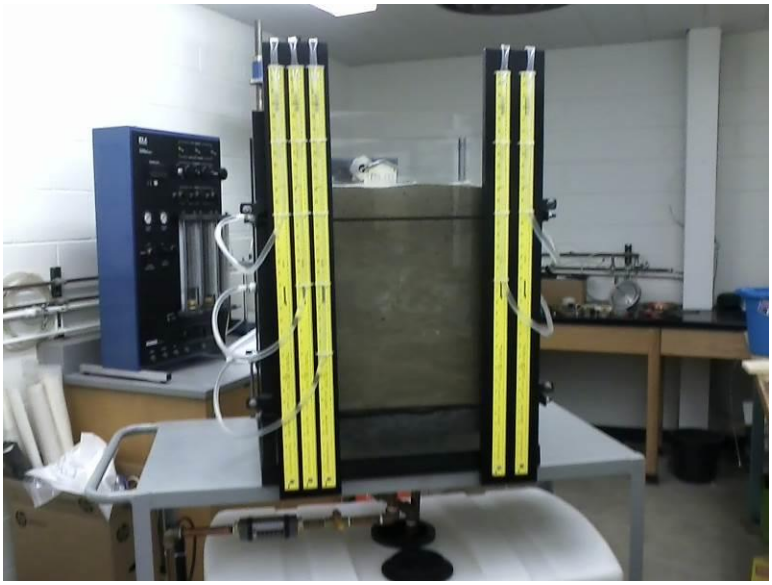

FIGURE 58. Piezometers attached to finalized liquefaction tank.

CHAPTER 4

TESTING AND CALCULATIONS

4.1 Sample Sand Criteria and Characteristics

There are certain criteria that must be met in order for liquefaction to occur. Generally, the sand needs to be relatively clean with a small percentage of fines, a high-water table, and an external force to cause a sufficient increase in pore water pressures to trigger liquefaction. Ottawa sands have been commonly researched in the past due to relatively clean coarse grain sand which can be brought to liquefaction relatively easily. Different locations around the world with different sands have had damages to structures due to this phenomenon. Local sands in the city of Long Beach were researched for liquefaction potential prior to choosing a sand for the tank. This was done to make this phenomenon more relatable to locals in the Southern California region.

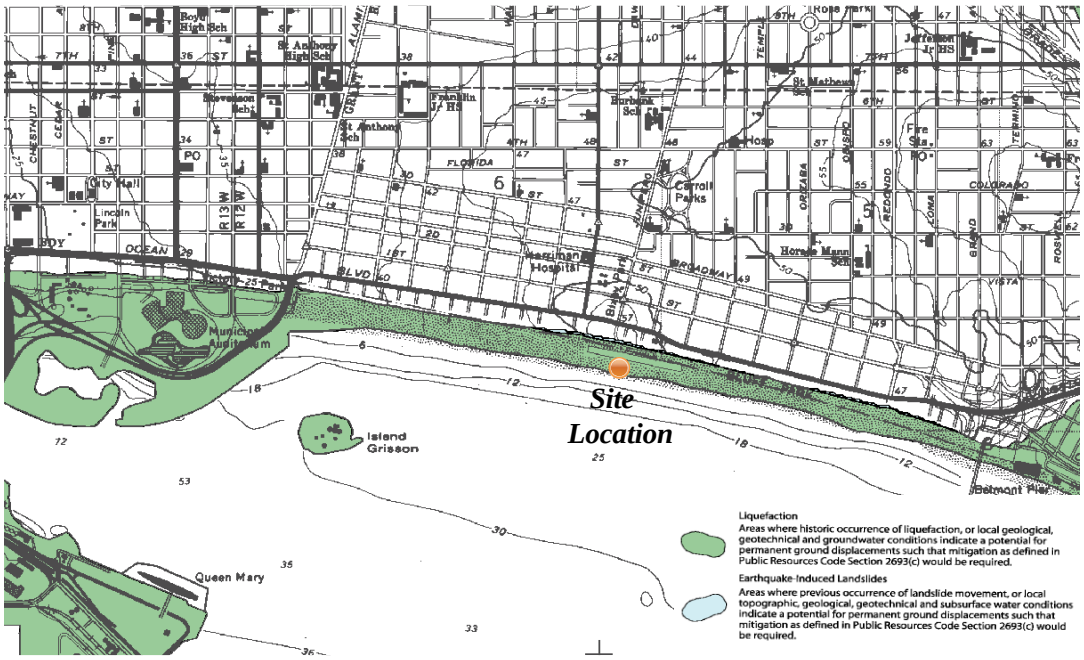

FIGURE 59. Liquefaction hazards zones (California Department of Conservation 1999).

Long Beach Quadrangle Seismic Hazard Zones map from the California Division of Mines and Geology was used to determine zones around the city of Long Beach that may be prone to liquefaction. This map shows that probability of seismically induced liquefaction is situated mostly near waterway areas. These areas include the Port of Long Beach, Los Angeles River, San Gabriel River, Belmont Shore, Alamitos Bay, and all the beachfront along Ocean Boulevard.

A sample of Long Beach sand was collected from the beachfront by Ocean Boulevard and Junipero Avenue, also known as Junipero Beach, as shown in Figure 59. Sieve analysis were conducted on this type of soil and its gradation is plotted on the grain size distribution boundaries for liquefiable soil, as shown in Figure 60 (Tsuchida 1970). This grain size distribution falls within the boundaries for most liquefiable soils based on grain size distribution. The sand for the liquefaction tank were collected at this location.

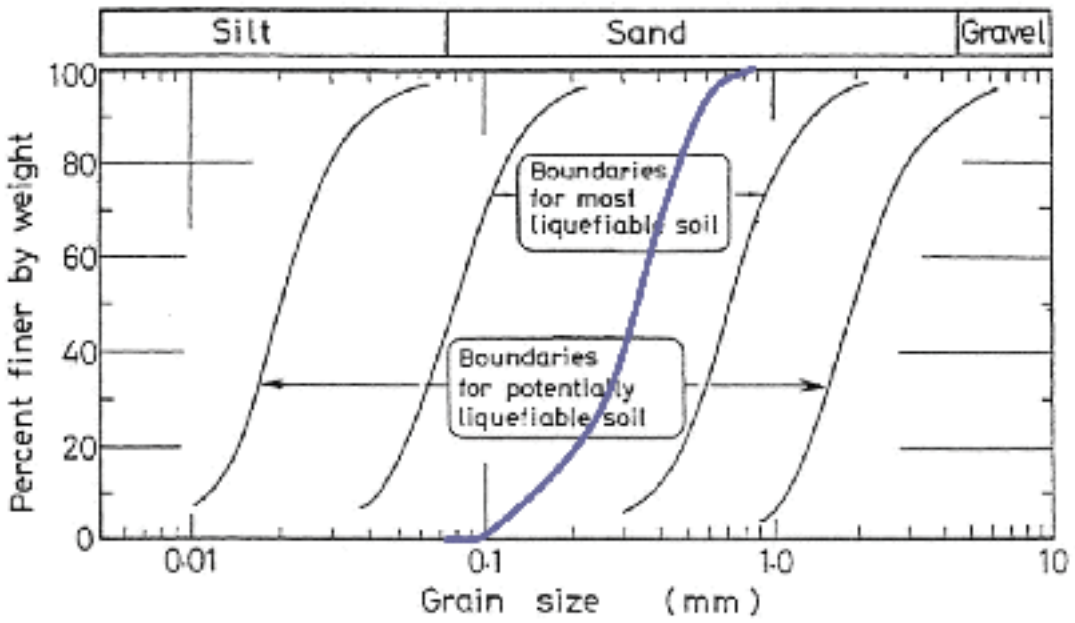

FIGURE 60. Grain size distribution of the obtained sample (Tsuchida 1970).

TABLE 1. Properties of Long Beach Sand Collected at Junipero Beach

Sand Properties		
D_{10}	=	0.28 mm
D_{30}	=	0.55 mm
D_{60}	=	1.5 mm
C_u	=	5.36
C_c	=	0.72
e_{max}	=	0.91
e_{min}	=	0.61
G_s	=	2.64

Long Beach sand collected at this location has a particle diameter at 10% finer by mass (D_{10}) of 0.28mm, a particle diameter at 30% finer by mass (D_{30}) of 0.55mm, a particle diameter at 60% finer by mass (D_{60}) of 1.5mm, a coefficient of uniformity (C_u) of 5.36, a coefficient of curvature (C_C) of 0.72, maximum void ratio (e_{max}) of 0.906, minimum void ratio (e_{min}) of 0.614, and a specific gravity of 2.637, as shown in Table 1 (Ortiz 2017).

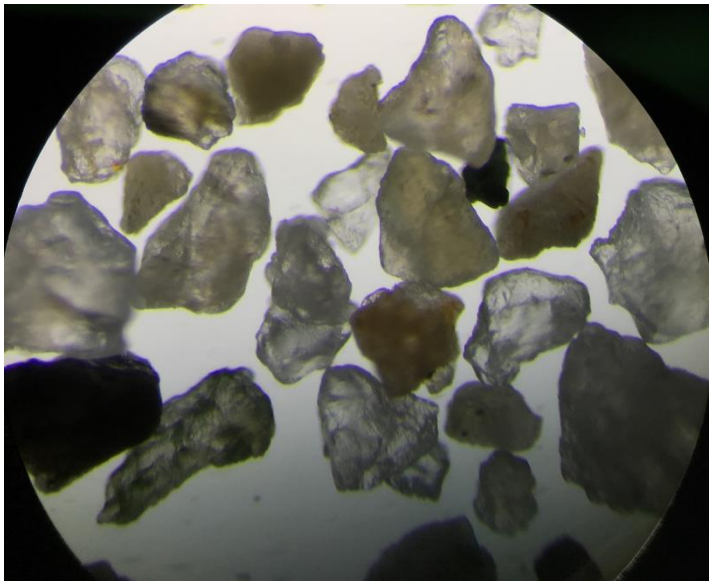

FIGURE 61. Light microscopic view of Long Beach sand sample.

This sand is classified as a poorly graded sand with a composition of sub angular sand grains, as shown Figure 61 (Ortiz 2017). The sands collected were cleaned prior to placing them

in the tank. They were first sieved through sieve #4 to remove any debris. After, the sands were wet sieved through sieve #200 to remove as much fines as possible to allow a clear view of liquefaction as it occurs.

4.2 Testing Procedure

The steps suggested for the testing procedure and liquefaction demonstration with this tank are as follows:

1. Close the red drain valve and fully open the yellow valve.
2. Turn on the pump.
3. Adjust the flowrate to 15 liters per minute by adjusting the yellow valve. Note: Leaving the valve fully open can cause a water/sand mixture to gush over the top of the tank.
4. Fill the tank with water up to the top of the sand layer.
5. Turn off the pump and fully close the yellow valve to prevent water backflow through the pump.
6. Let the sand become fully saturated by waiting 24 hours.
7. Remove any entrapped pockets of air inside the piezometers.
8. Loosen sands by mechanical method.
9. Place model building on top of sand layer taking care not to densify the soils by driving it into the soil.
10. Hit the side of the liquefaction tank with your palm or rubber mallet.
11. Observe for signs of liquefaction, model building sinking into the soil layer, and record piezometer readings. If no liquefaction was observed, impact the tank with greater force. If liquefaction is still not observed, continue with Step 8.

It is important to note that liquefaction is not always guaranteed under laboratory conditions. The major factors that prevents liquefaction from being achieved under the proposed laboratory conditions is the saturation level and relative density of the sands. Difficulty can arise in achieving liquefaction if the soils are partially saturated caused by entrapped gas within the soil mass that dampens the impact force during testing. Over time and testing the soil densifies and it becomes more difficult to achieve liquefaction. The sands must be loosened to achieve liquefaction. Loosening of the sands can be accomplished by filling the tank with water up to the surface and using a long rod to stir the soils in circular motions across the whole tank. As the soils loosen, less effort will be required to stir the whole mixture.

4.3 Soil Strength Calculations

It was observed that liquefaction occurred during the testing procedure with an average increase in piezometric readings between 5 cm to 10 cm. The Mohr-Coulomb failure criterion was used to calculate effective stresses and shear strength values at average piezometric readings where liquefaction was observed, as shown in Table 2. A saturated unit weight of 19.6 kN/m^3 and friction angle of 33° was used for the calculations. Soil cohesion was assumed to be zero due to very low fine contents. From these calculations, it can be seen that as the dynamic load increases, the excess pore water pressure (u) also increases. The buildup of excess pore water pressure causes the effective stresses (σ'**)** of the sand to decrease and in turn the shear strength (τ') to be reduced. The shear strength of the soil is momentarily lost in the upper 10 cm when the dynamic load is applied. It is during this stage when the shear strength is negligible and liquefaction is observed as the model building sinks into the soil layer.

TABLE 2. Theoretical Calculations for Observed Liquefaction Between 5 cm to 10 cm Increase of Water Column Head

		At Rest Condition			Piezometer = +5 cm			Piezometer = +10 cm		
Depth (cm)	**σ (kPa)**	**u (kPa)**	**σ' (kPa)**	**τ' (kPa)**	**$u_{2"}$ (kPa)**	**$\sigma'_{2"}$ (kPa)**	**$\tau'_{2"}$ (kPa)**	**$u_{4"}$ (kPa)**	**$\sigma'_{4"}$ (kPa)**	**$\tau'_{4"}$ (kPa)**
0	0	0	0	0	0	0	0	0	0	0
2.54	0.50	0.25	0.25	0.16	0.75	L	L	1.23	L	L
5.08	1.00	0.50	0.50	0.32	1.00	L	L	1.48	L	L
7.62	1.50	0.75	0.75	0.49	1.24	0.25	0.16	1.73	L	L
10.16	1.99	1.00	1.00	0.65	1.49	0.50	0.33	1.98	L	L
12.70	2.49	1.24	1.25	0.81	1.74	0.75	0.49	2.22	0.27	0.17
15.24	2.99	1.49	1.50	0.97	1.99	1.00	0.65	2.47	0.52	0.34
17.78	3.49	1.74	1.75	1.14	2.24	1.25	0.81	2.72	0.77	0.50
20.32	3.99	1.99	2.00	1.30	2.49	1.50	0.97	2.97	1.02	0.66
22.86	4.49	2.24	2.25	1.46	2.74	1.75	1.14	3.22	1.27	0.82
25.40	4.99	2.49	2.50	1.62	2.99	2.00	1.30	3.47	1.52	0.99
27.94	5.48	2.74	2.75	1.78	3.24	2.25	1.46	3.72	1.77	1.15
30.48	5.98	2.99	3.00	1.95	3.48	2.50	1.62	3.97	2.02	1.31

Note: L = Liquefiable soil

CHAPTER 5

CONCLUSION AND FUTURE STUDIES

5.1 Summary

Different models of liquefaction tanks have been built and used by educational institutions for demonstrative and research applications. Those liquefaction tanks proved to be successful in simulating liquefaction in loose sandy soils like the one collected from Long Beach. This liquefaction tank can be used for educational purposes about the liquefaction phenomenon and can be used to conduct future research on liquefaction mitigation.

5.2 Limitations and Future Improvements

There are some limitations that the author came across when conducting testing on the liquefaction tank. One of these limitations is that there is not a pore pressure transducer to accurately measure pore water pressures on the liquefaction onset or dissipation during the post-liquefaction stage. The current piezometers work, but do not have the ability to record variations of pore water pressures with time. A future improvement is to install pore pressure transducers to overcome this limitation.

A rubber mallet is currently being used to induce liquefaction. Although this method works in inducing liquefaction for demonstrative purposes, the force inputted into the systems is unknown and can only be estimated by back calculation. A better system must be installed so that a force controlled device can be used for future research applications.

5.3 Future Studies

Engineers have been looking for ways to mitigate and prevent liquefaction from occurring since the discovery and documentation of this phenomenon. It is known that liquefaction generally occurs in loose sandy soils that are fully saturated. Previous research has

shown that partially saturated soils have larger liquefaction resistance. Future studies can take this into account and conduct research into implementing methods to reduce the degree of saturation. Such method may include the injection of gas into soil to reduce saturation levels and study the long-term effectiveness.

Previous research has also shown that the denser the sandy soil, the greater the liquefaction resistance. Older deep natural soil deposits tend to have a natural cementation that prevent liquefaction. Younger soil deposits near the surface are generally loose and more prone to liquefaction. Mechanical methods have already been developed to densify liquefiable soils and help to speed up the process. An alternative microbiological method has been developed that uses bacteria to increase the shear strength of soil through a process called biocementation. Biocementation is a field of research that is being studied as a potential ground improvement technique. Bacteria is used to induce calcium carbonate ($CaCO_3$) on a soil structure to cement soil particles. Previous research conducted by Lin et al. (2015, 2016), showed the improvements of soil strength using this ground improvement method. Through this research, it was shown that the soil strength of the bacteria treated soil increased. It was also shown that the axial compressive response of porous piles in soil treated with bacteria increased. A future area of study is to expand those findings to the response of laterally loaded piles in biocemented soils. The current liquefaction tank can be modified to study this problem. Such modifications may include refilling the water reservoir with a biogrouting bacterial solution, removing the piezometers and replacing them with plugs to keep all the bacterial solution inside the tank, installing a top cap for the tank to hold a pile in place and seal the containing vessel, the installation of a lateral loading system, pressure cells, and bender elements.

This liquefaction tank can also be used for future laboratory demonstrations. Northwestern University has used their liquefaction tank for laboratory demonstrations and have develop a laboratory guide and worksheet to accompany the laboratory activity. A sample of the laboratory worksheet is included in the “APPENDIX”. The Quicksand Laboratory manual gives the procedure to conduct a laboratory exercise for quicksand conditions and liquefaction testing. This example serves as a guide to develop a future laboratory assignment that incorporates the liquefaction tank into a civil engineering laboratory exercise.

APPENDIX

QUICKSAND LABORATORY MANUAL

Quicksand Laboratory

Purpose

A sand layer depending upon its relative density and degree of saturation behaves differently under static and dynamic loading. The direction and the rate of water flow also plays an important role in this behavior. The purpose is to observe the changes in the properties of a san layer due to above mentioned condition using a sand tank model.

Procedure

1. Record the thickness of the sand layer and the height of the water levels in the tank and in the piezometric tubs at the initial condition where the sand layer is loose and saturated with no water flow.

2. Let the water flow in an upward direction and slowly increase the flow rate. Record the water levels in the piezometric tubes with respect to flow rates and observe the change in the behavior of the sand layer as the flow rate increases.

3. When the sand layer is in the quick condition observe which objects can sink and which can float on the sand surface.

4. Turn off the water flow in an upward direction and let the water drain out in a downward direction. Try to dig a hole in the sand and observe what happens to its slopes when the drainage is cut off.

5. Drain the water out until the water level is slightly below the sand surface. Record the water levels in the piezometers and in the tank at constant intervals during the whole process.

6. Apply slowly increasing pressure with the palm of the hand to the top of the sand layer until failure or quick condition occurs. Record the change of water levels at the piezometers and observe what happens to the sand layer and record its thickness.

7. Drain out the water collected at the top of the sand layer until water level is slightly below sand surface. Repeat the step 6.

8. Repeat the step 7 and 6 until failure or quick condition cannot be achieved by static loading.

9. Place the little model of the house on the sand surface and hit the side of the tank with the hand or the rubber hammer. Record the sudden changes in the piezometers and observe what happens to the house and to the sand layer. Record the final thickness of the sand layer.

10. Repeat the step 9 until it is too hard to achieve the quick condition.

11. Repeat the steps 1 and 2 starting with denser sand.

Calculations and Discussion

1. Explain and discuss briefly what happens during each step of the experiment.

2. Calculate critical gradients $i_{cr} = (G_s-1)/(1+e)$ and compare with experimental results $i_{cr}=\Delta h/L$, $\Delta h=h_2-h_1$.

3. Calculate void ratios after each quick condition and for both tests.

4. Calculate hydraulic gradients for corresponding flow rates in Step 2 and plot $\Delta h/L$ versus flow rate for both tests.

Questions

1. What is the most probable reason for the difference between the calculated and measured values for the critical gradient?

2. What would have been the effect on the critical gradient if we had left the sand more loosely packed at the beginning of our experiment?

3. What would have been the effect on the flow rate at which the quick condition occurred if the sand had been more loosely packed?

4. What would have been the effect on the critical gradient if we had used a finer sand?

5. What would have been the effect on the flow rate at which the quick condition occurred if we had used finer sand?

Name: _____ Sample & Test Number: _____

Date: _____ Sheet Number: _____

Quicksand Experiment

Weight of solids W_s = _____ kg Volume of Solids = _____ m^3

Specific Gravity of solids G = _____ Area of Tank = _____ m^2

No.	Flow, L/min	Pipette Readings (cm)			Sand Depth (cm)					L' (cm)	i = Δh/ L	Velocity, cm/s	Volume, A*L, m^3	Volume Voids, m^3	Void Ratio, e	i_c= Critical gradient	k, cm/s	T, C°	k_{20}, cm/s
		1	2	Avg., Δh	1	2	3	4	Avg., = L										
1																			
2																			
3																			
4																			
5																			
6																			
7																			
8																			
9																			
10																			
11																			
12																			
13																			
14																			
15																			
16																			
17																			
18																			
19																			
20																			

REFERENCES

REFERENCES

Bartlett, S.F., and Youd, T.L. (1992). *Empirical analysis of horizontal ground displacement generated by liquefaction-induced lateral spread.* National Center for Earthquake Engineering Research, Buffalo, NY.

Bray, J. D., Rourke, T. D. O., Cubrinovski, M., Zupan, J. D., Taylor, M., Toprak, S., Hughes, M., and Ballegooy, S. Van. (2013). *Liquefaction impact on critical infrastructure in Christchurch*. Geological Survey Research Report, Ithaca, NY.

California Department of Conservation (1999). "U.S. Seismic Design Maps." <http://earthquake-.usgs.gov/designmaps/us/application.php> (July, 2016).

California Department of Conservation (2016). "Regulatory Maps."<http://maps.conservation.-ca.gov/cgs/informationwarehouse/index.html?map=regulatorymaps> (July, 2016).

Casagrande, A. (1936). "Characteristic of cohesionless soils affecting the stability of slopes and earth fills." *Journal of the Boston Society of Civil Engineers*, 1, 257–276.

Heidari, T. (2012). "Liquefaction potential assessment of Pleistocene beach sands near Charleston, South Carolina." *J.Geotech.Geoenviron.Engineering*, 138(10), 1196-1208.

Holtz, R. D., Kovacs, W. D., and Sheahan, T. C. (2010). *Introduction to geotechnical engineering*, 2nd Ed., Prentice Hall, Upper Saddle River, NJ.

Hryciw, R. (1985). "Geotextile filters for a large liquefaction tank." *Geotech Test J,* 8(3), 140-142.

Hu, H. (2009). "Research on earthquake response of sandy soil and preventative measures of liquefaction in Xiamen." *Journal of Harbin Institute of Technology*, 16(1), 19-22.

Kiyota, T. (2014). "Mitigation of liquefaction-induced damage to residential houses by shallow ground improvement." *Soil liquefaction during recent large-scale earthquakes-selected papers from the New Zealand: Japan Workshop on soil liquefaction during recent large-scale earthquakes*, 157-166.

Kramer, S. (1996). *Geotechnical earthquake engineering*, 1st Ed., Prentice-Hall, Upper Saddle River, NJ.

Landers, J. (2012). "New method for alleviating soil liquefaction to undergo field tests." *Civil Engineering*, 82(5), 38.

Lin, H, Suleiman, M., Brown, D., and Kavazanjian, E. (2015). "Mechanical behavior of sands treated by microbially induced carbonate precipitation." *Journal of Geotechnical and Geoenvironmental Engineering*, 142(2), 04015066.

Lin, H. Suleiman, M., Jabbour, H., Brown, D., and Kavazanjian, E. (2016). “Enhancing the axial compression response of pervious concrete ground improvement piles using biogrouting.” *Journal of Geotechnical and Geoenvironmental Engineering*, 142(10), 04016045.

Maurer, B. (2014). "Evaluation of the liquefaction potential index for assessing liquefaction hazard in Christchurch, New Zealand." *Journal of Geotechnical and Geoenvironmental Engineering*, 140(7), 04014032.

Ortiz, J. (2017). “Soil characterization of biocemented Long Beach sand.” Master Thesis, California State University Long Beach. Under preparation.

Pande, G. N. (2008). "Assessment of risk of liquefaction in granular materials and its mitigation." *Proc. 12th International Conference on Computer Methods and Advances in Geomechanics (IACMAG)*, Goa, India (pp. 2619-2627).

Seed, R. B., Riemer, M. F., and Dickenson, S. E. (1989). “Liquefaction of soils in the 1989 Loma Prieta earthquake.” *Proc. International Conferences on Recent Advances in Geotechnical Earthquake Engineering and Soil Dynamics*, 9.

Tokimatsu, K., Kojima, H., Kuwayama, S., Abe, A., and Midorikawa, S. (1994). “Liquefaction-induced damage to buildings in 1990 Luzon earthquake.” *Journal of Geotechnical Engineering*., 120(2), 290-307.

Tsuchida, H (1970). “Predictions and countermeasure against the liquefaction in sand deposit.” Abstract of the seminar in the Port and Harbor Research Institute, Yokohama, (pp.3.1-3.3).

Yasuda, S. (2014). "New liquefaction countermeasures for wooden houses." *Soil liquefaction during recent large-scale earthquakes - selected papers from the New Zealand: Japan Workshop on soil liquefaction during recent large-scale earthquakes*, 167-179.

Zeng, X. (2005). “Effect of liquefaction on stability walls.” <http://ascelibrary.org/doi/pdf/10.-1061/40779%28158%2919> (May, 2016).